Article

Effect of Protons on the Optical Properties of Oxide Nanostructures

Markus Mller, Slavica Stankic, Oliver Diwald, Erich Knzinger,
Peter V. Sushko, Paolo E. Trevisanutto, and Alexander L. Shluger

J. Am. Chem. Soc., **2007**, 129 (41), 12491-12496• DOI: 10.1021/ja0736055 • Publication Date (Web): 25 September 2007

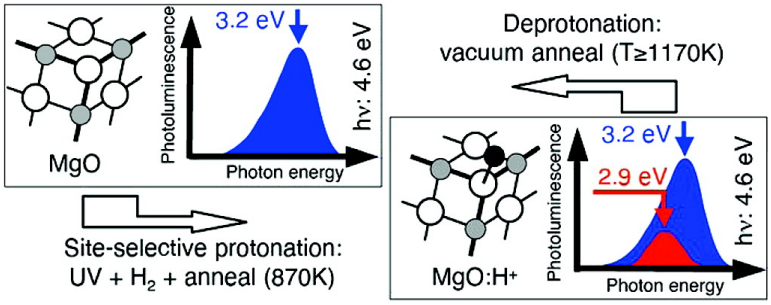

More About This Article

Additional resources and features associated with this article are available within the HTML version:

- Supporting Information
- Links to the 4 articles that cite this article, as of the time of this article download
- Access to high resolution figures
- Links to articles and content related to this article
- Copyright permission to reproduce figures and/or text from this article

View the Full Text HTML

J|A|C|S
ARTICLES
Published on Web 09/25/2007

Effect of Protons on the Optical Properties of Oxide Nanostructures

Markus Müller,[†] Slavica Stankic,[†] Oliver Diwald,*[,†] Erich Knözinger,[†] Peter V. Sushko,*[,‡] Paolo E. Trevisanutto,[‡,§] and Alexander L. Shluger[‡]

Contribution from the Institute of Materials Chemistry, Vienna University of Technology, Veterinärplatz 1/GA, A-1210 Vienna, Austria, and Virtual Materials Laboratory, Department of Physics & Astronomy and London Centre for Nanotechnology, Materials Simulation Laboratory, University College London, Gower Street, London WC1E 6 BT, United Kingdom

Received May 19, 2007; E-mail: p.sushko@ucl.ac.uk; odiwald@mail.zserv.tuwien.ac.at

Abstract: Site-specific functionalization of oxide nanostructures gives rise to novel optical and chemical surface properties. In addition, it can provide deeper insights into the electronic surface structure of the associated materials. We applied chemisorption of molecular hydrogen, induced by ultraviolet (UV) light, followed by vacuum annealing to MgO nanocubes to selectively decorate three-coordinated oxygen ions (oxygen corner sites, for simplicity) with protons. Fully dehydroxylated nanocubes exhibit 3.2 ± 0.1 eV photoluminescence induced by 4.6 eV light, where both emission and absorption are associated with three-coordinated oxygen sites. We find that partially hydroxylated nanocubes show an additional photoluminescence feature at 2.9 ± 0.1 eV. Interestingly, the excitation spectra of the 2.9 and 3.2 eV emission bands, associated with protonated and nonprotonated oxygen corner sites, respectively, nearly coincide and show well-pronounced maxima at 4.6 eV in spite of a significant difference in their local atomic and electronic structures. These observations are explained with the help of ab initio calculations, which reveal that (i) the absorption band at 4.6 eV involves four-coordinated O and Mg ions in the immediate vicinity of the corner sites and (ii) protonation of the three-coordinated oxygen ions eliminates the optical transitions associated with them and strongly red-shifts other optical transitions associated with neighboring atoms. These results demonstrate that the optical absorption bands assigned to topological surface defects are not simply determined by the ions of lowest coordination number but involve contributions due to the neighboring atoms of higher coordination. Thus, we suggest that the absorption band at 4.6 eV should not be regarded as merely a signature of the three-coordinated O^{2-} ions but ought to be assigned to corners as multiatomic topological features. Our results also suggest that optical absorption signatures of protonated and nonprotonated sites of oxide surfaces can be remarkably similar.

1. Introduction

Recent years have seen an explosion in both experimental and theoretical research on nanoparticles and nanoscale objects. This research is driven by the promise of qualitatively new technological advances that may become possible once the properties of nanoparticles are understood and taken under control.[1−8] Significant progress has been achieved in the methods of nanoparticle synthesis with a huge diversity of forms, dimensions, and structures currently available.[9−11]

Optical properties of nanoparticles are of particular interest since it has long been noticed that characteristics of both absorption and emission can strongly depend on the size and shape of particles. In semiconducting materials such dependence is attributed to quantum confinement phenomena and determined by the particle dimensions. On the other hand, in the case of ionic materials, such as particles of nanostructured alkaline earth metal oxides,[12−16] the size-related modifications of the optical

[†] Vienna University of Technology.
[‡] University College London.
[§] Present address: Institut NEEL, CNRS, Grenoble, France.

(1) Wased, Y., Muramatsu, A., Eds. *Morphology Control of Materials and Nanoparticles—Advanced Materials Processing and Characterization*; Springer-Verlag: Berlin, 2004.
(2) Xia, Y. N.; Yang, P. D.; Sun, Y. G.; Wu, Y. Y.; Mayers, B.; Gates, B.; Yin, Y. D.; Kim, F.; Yan, Y. Q. *Adv. Mater.* **2003**, *15*, 353.
(3) Erwin, S. C.; Zu, L.; Haftel, M. I.; Efros, A. L.; Kennedy, T. A.; Norris, D. J. *Nature* **2005**, *436*, 91.
(4) Burda, C.; Chen, X. B.; Narayanan, R.; El-Sayed, M. A. *Chem. Rev.* **2005**, *105*, 1025.
(5) Roan, J.-R. *Phys. Rev. Lett.* **2006**, *96*, 248301.
(6) Shevchenko, E. V.; Talapin, D. V.; Murray, C. B.; O'Brien, S. *J. Am. Chem. Soc.* **2006**, *128*, 3620.
(7) Riss, A.; Berger, T.; Grothe, H.; Bernardi, J.; Diwald, O.; Knözinger, E. *Nano Lett.* **2007**, *7*, 433.
(8) Urban, J. J.; Uuyang, L.; Jo, M.-H.; Wang, D. S.; Park, H. *Nano Lett.* **2004**, *4*, 1547.
(9) Song, O.; Zhang, Z. J. *J. Am. Chem. Soc.* **2004**, *126*, 6164.
(10) Zhu, K. K.; Hu, J. C.; Kubel, C.; Richards, R. *Angew. Chem., Int. Ed.* **2006**, *45*, 7277.
(11) Hao, Y.; Meng, G.; Ye, C.; Zhang, X.; Zhang, L. *J. Phys. Chem. B* **2005**, *109*, 11204.
(12) Dohnalek, Z.; Kimmel, G. A.; McCready, D. E.; Young, J. S.; Dohnalkova, A.; Smith, R. S.; Kay, B. D. *J. Phys. Chem. B* **2002**, *106*, 3526.
(13) Goniakowski, J.; Noguera, C.; Giordano, L. *Phys. Rev. Lett.* **2004**, *93*, 215702.
(14) Mel'gunov, M. S.; Fenelonov, V. B.; Mel'gunova, E. A.; Bedilo, A. F.; Klabunde, K. J. *J. Phys. Chem. B* **2003**, *107*, 2427.
(15) Stankic, S.; Bernardi, J.; Diwald, O.; Knözinger, E. *J. Phys. Chem. B* **2006**, *110*, 13866.
(16) Stankic, S.; Bernardi, J.; Diwald, O.; Knözinger, E. *J. Phys. Chem C* **2007**, *111*, 8069−8074.

absorption spectra are defined by the relative concentration of low-coordinated surface ions.[17,18] For example, the optical absorption at 4.6 eV, which is assigned to three-coordinated oxide ions, is undetectable in 10 nm MgO nanoparticles. However, it develops into a pronounced band in 5 nm particles and strongly gains in intensity in 3 nm particles.[17] In addition, further modifications of the optical properties can be caused by the atomistic structure of interfaces between different nanoparticles.[19]

First studies demonstrating the correspondence between coordination number of surface sites and their optical properties, have been carried out by Zecchina and co-workers.[20−22] They have used highly dispersed MgO, CaO, SrO, and BaO powders with different concentrations of three-, four-, and five-coordinated oxygen anion sites to identify optical absorption bands associated with the sites of each coordination. Their predictions have been later confirmed by theoretical ab initio calculations.[23] However, as we show below, some important details regarding the nature of the optical transitions have been overlooked due to technical limitations of the time.

Since nanoparticles have a large number of surface atoms, as compared to bulk crystalline samples, and, in general, a complex surface topology, the assignment of their spectroscopic features is not straightforward. One of the possible routes to unambiguously identifying the nature of the optical transitions associated with each surface structure is to consider the dependence of the optical properties on the size of the particles.[17] A complementary route involves a nondestructive modification of the particles which would allow one to selectively induce and control optical processes associated with various structural features. One of the usual approaches to achieving this is doping. For example, doping of MgO nanoparticles with a small amount of Ca drastically affects both the energy and the intensity of the photoluminescence.[18] However, this methodology has certain disadvantages: doping is a nonreversible process and it is rarely site-selective. Alternatively, to control the spectroscopic properties of particular structural features, one can chemically modify the sample surface so that, for example, to decorate low-coordinated surface ions, which are expected to contribute to light absorption and emission. This can be achieved via adsorption of atoms or molecules that selectively bind to sites of interest[24−29] and alter their electronic structure and, thus, their optical properties.

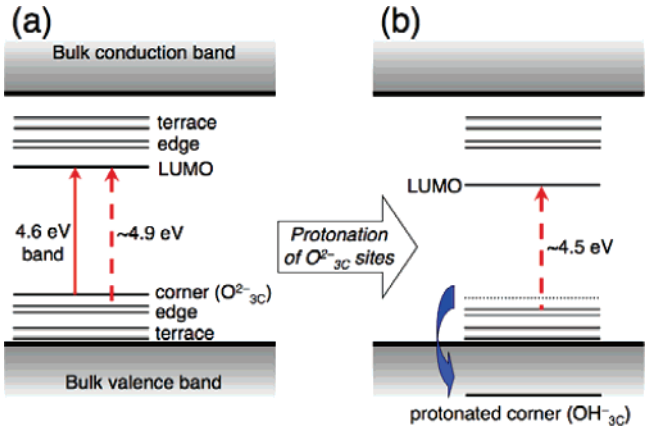

Figure 1. Schematics of the electronic structure of an oxygen-terminated corner in MgO nanoparticle before (a) and after (b) the protonation of the three-coordinated O^{2-} site. Horizontal lines show energy levels and subbands associated with surface structural features. Vertical arrows indicate the optical transitions between the occupied and lowest unoccupied (LUMO, see text below) states of the system.

In the present work we applied this approach to 3−10 nm MgO nanocubes, which comprise sharp edges and particularly high concentrations of three-coordinated (3C) sites,[17,30] which exhibit high absorption intensity at photon energies above ~4 eV. Moreover, these particles have high thermal stability, which allows us to target specifically anion sublattice by site-selectively and reversibly protonating them. We note that there is considerable interest in characterization of not only optical but also vibrational[31] and electronic[32] properties of hydroxyl groups at the surface of oxide nanostructures.

Previous experimental and theoretical studies firmly assigned the optical absorption band at 4.6 eV and the corresponding photoluminescence (PL) band at 3.2 ± 0.1 eV to 3C oxygen sites. This absorption energy is much lower than the energy of the bulk excitation due to a splitting of the occupied and unoccupied energy levels from the bulk band edges, as shown in Figure 1a. The same effect determines the absorption energies due to four- and five-coordinated sites for which both experimental and theoretical results suggest the values close to 5.7 and 6.2 eV, respectively.[22,23,33] Protonation of the 3C sites[34,35] shifts both occupied and unoccupied states in the vicinity of the proton site to lower energies, as illustrated in Figure 1b. This affects most strongly the 2p states of the hydroxylated 3C oxygen and the shift decreases in magnitude with increasing distance from the proton site. Therefore, we expect that the protonated corners will have no optical absorption in the region of 4.6 eV and no corresponding photoluminescence. Instead, we observed that hydroxylated surfaces exposed to 4.6 eV light exhibit an additional intense PL band at 2.9 ± 0.1 eV. Moreover, this emission band has essentially the same excitation spectrum as that of the emission band assigned to nonprotonated 3C sites, in spite of the strong perturbation of the electronic structure of the 3C site induced by its protonation.

(17) Stankic, S.; Müller, M.; Sterrer, M.; Bernardi, J.; Diwald, O.; Knözinger, E. *Angew. Chem., Int. Ed.* **2005**, *44*, 4917.
(18) Stankic, S.; Sterrer, M.; Hofmann, P.; Bernardi, J.; Diwald, O.; Knözinger, E. *Nano Lett.* **2005**, *5*, 1889.
(19) McKenna, K. P.; Sushko, P. V.; Shluger, A. L. *J. Am. Chem. Soc.* **2007**, *129*, 8600.
(20) Zecchina, A.; Stone, F. S. *J. Chem. Soc., Faraday Trans. I* **1976**, *72*, 2364.
(21) Zecchina, A.; Lofthouse, M. G.; Stone, F. S. *J. Chem. Soc., Faraday Trans. I* **1975**, *71*, 1476.
(22) Garrone, E.; Zecchina, A.; Stone, F. S. *Philos. Mag.* **1980**, *42 B*, 683.
(23) Shluger, A. L.; Sushko, P. V.; Kantorovich, L. N. *Phys. Rev. B* **1999**, *59*, 2417.
(24) Coluccia, S. In *Adsorption and Catalysis on Oxide Surfaces*; Che, M., Bond, G. C., Eds.; Elsevier: Amsterdam, 1984.
(25) Chiesa, M.; Giamello, E.; Di Valentin, C.; Pacchioni, G.; Sojka, Z.; Van Doorslaer, S. *J. Am. Chem. Soc.* **2005**, *127*, 16935.
(26) Anpo, M.; Che, M. *Adv. Catal.* **1999**, *44*, 119.
(27) Bailly, L.-M.; Costentin, G.; Lauron-Pernot, H.; Krafft, J. M.; Che, M. *J. Phys. Chem. B* **2005**, *109*, 2404.
(28) Hacquart, R.; Krafft, J.-M.; Costentin, G.; Jupille, J. *Surf. Sci.* **2005**, *595*, 172.
(29) a) Chiesa, M.; Paganini, M. C.; Giamello, E. *ChemPhysChem* **2004**, *5*, 1897. (b) Chiesa, M.; Paganini, M. C.; Giamello, E.; Di Valentin, C.; Pacchioni, G. *ChemPhysChem* **2006**, *7*, 728.
(30) Spoto, G.; Gribov, E. N.; Ricchiardi, G.; Damin, A.; Scarano, D.; Bordiga, S.; Lamberti, C.; Zecchina, A. *Prog. Surf. Sci.* **2004**, *76*, 71.
(31) Chizallet, C.; Costentin, G.; Che, M.; Delbecq, F.; Sautet, P. *J. Am. Chem. Soc.* **2007**, *129*, 6442.
(32) Napoli, F.; Chiesa, M.; Giamello, E.; Finazzi, E.; Di Valentin, C.; Pacchioni, G. *J. Am. Chem. Soc.* **2007**, *129*, 10575−10581.
(33) Cox, P. A.; Williams, A. A. *Surf. Sci.* **1986**, *175*, L782.
(34) Sterrer, M.; Berger, T.; Diwald, O.; Knözinger, E.; Sushko, P. V.; Shluger, A. L. *J. Chem. Phys.* **2005**, *123*, 064714.
(35) Diwald, O.; Sterrer, M.; Knözinger, E. *Phys. Chem. Chem. Phys.* **2002**, *4*, 2811.

Understanding how the protonation of oxygen 3C sites modifies the photoemission of MgO nanoparticles and explaining the similarity of PL excitation spectra obtained for protonated and nonprotonated oxygen corners will be useful for elucidating spectroscopic properties of protonated oxide surfaces. By combining experimental and theoretical techniques, we found that optical absorption energies of surface sites are determined not only by the coordination number of the corresponding lattice ions but also by their relative position with respect to the surface topological defects. In particular, optical transitions associated with four-coordinated O^{2-} (4C) ions located in the vicinity of the corners can be excited with the energies of 4.8 eV, which is significantly lower than the absorption energy of 5.7 eV usually attributed to 4C ions on MgO steps. Thus, optical absorption signature of these sites is similar to that of 3C sites, while their chemical properties are in line with those of other 4C sites. Furthermore, we found that protonation of three-coordinated O^{2-} ions changes the nature of optical absorption in two respects. First, the energy levels of the 3C O^{2-} ion shift deep into the bulk valence band and, consequently, the energies of the corresponding optical transitions shift from ~4.6 eV up to much higher values. Second, the energies of optical transitions due to neighboring 4C O^{2-} ions shift to lower values of 4−4.5 eV so that the absorption intensity in the low-energy part of the spectrum is only slightly affected (see Figure 1).[36] Our results suggest that optical absorption signatures of protonated and nonprotonated surface sites can be remarkably similar in spite of a dramatic difference in their local atomic and electronic structures and chemical properties. Similar effects are expected in other oxide nanostructures.

2. Experimental Section

MgO nanocrystals were prepared by the chemical vapor deposition technique (CVD) based on the metal vapor combustion with oxygen within a flow reactor system. The details of this technique are given elsewhere.[37] Then the sample material was subjected to thermal treatment. First, the sample was cleaned of organic contaminants by heating it at a rate of 5 K·min^{-1} to 873 K and exposing it to oxygen. Then the sample temperature was raised to 1173 K at pressures $p < 5 \times 10^{-6}$ mbar and kept at this temperature for 1−2 h until full dehydroxylation of the sample surface was achieved as judged by IR spectroscopy.[35] The IR experiments were performed in a cell that allows for sample activation at high-vacuum conditions with a base pressure below 5×10^{-6} mbar. Samples in the form of hand-pressed, self-supporting wavers were measured in the IR transmission mode with a Bruker 113v spectrometer. A total of 300 scans were accumulated for one spectrum to obtain a reasonable signal-to-noise ratio with a spectral resolution of 3 cm^{-1}. Photoluminescence and UV diffuse reflectance measurements were carried out at room temperature using quartz glass cells which guarantee vacuum conditions better than $p < 10^{-6}$ mbar. The UV-diffuse reflectance spectra were acquired using a Perkin-Elmer Lambda 15 spectrophotometer, equipped with an integrating sphere, and then converted to absorption spectra via the Kubelka−Munk transform procedure. A pulsed Xe discharge lamp served as an excitation light source in a Perkin-Elmer LS 50B system for photoluminescence measurements. The band intensities of the observed emission features were obtained using the GRAMS software package for curve fitting.[38] To check the reliability of the fitting procedure, we varied the position of the simulation band maxima. This only reduced the quality of the fit, but did not change the position of the derived excitation maxima.

3. Details of Theoretical Calculations

The electronic structure and optical absorption of pure and hydroxylated MgO nanocubes were investigated using an embedded cluster approach, which combines a quantum-mechanical treatment of a "region of interest" with a classical shell model treatment of the rest of a system. This approach, as implemented in the computer code GUESS (Gaussians Used for Embedded Systems Studies), has been described elsewhere.[39−41] In this work, an MgO powder particle is represented using a cubic nanocluster of $10 \times 10 \times 10$ ions, which is divided into three regions: (i) the "region of interest", which includes atoms considered quantum mechanically (QM cluster), (ii) a polarizable classical environment represented using interatomic potentials and the shell model,[42] and (iii) the interface between them. The total energy of the system includes the contributions due to the energy of the QM cluster in the external electrostatic potential due to the rest of the system, the interaction of the classical atoms with each other and with the atoms of the QM cluster and the interface. The total energy of the system is minimized with respect to the coordinates of all centers of the nanocluster, i.e., classical cores and shells as well as atoms of the QM cluster. The energy minimization is carried out until the change in the total energy, displacements of atoms, and the forces acting on these atoms become less than 10^{-5} eV, 0.0003 Å, and 0.003 eV·Å^{-1}, respectively.

To study the properties of an oxygen-terminated corner and its surroundings, we used a stoichiometric QM cluster $Mg_{13}O_{13}$ shown in Figures 6 and 7. The quantum-mechanical contributions to the total energy were calculated using the Gaussian 98 package[43] for ab initio calculations of molecules and a hybrid density functional B3LYP. The latter combines Becke's[44] exchange functional with 20% contribution of the exact exchange interaction with a correlation functional by Lee, Yang, and Parr.[45] The excitation energies were calculated using the time dependent density functional theory (TD-DFT) as implemented in the Gaussian 98 package. Oxygen and magnesium atoms of the QM cluster were described using Pople's standard 6-31G and LANL2DZ[46] basis sets, respectively, while a cc-pVDZ basis set was used for hydrogen atoms. The interface between the QM cluster and the remaining part of the system includes 48 Mg ions, denoted as Mg^*_{48} thereafter, and represented using an effective core pseudopotential (ECP).[46] The calculated excitation energies reported in this work are only slightly affected if more flexible basis sets and larger QM clusters are used, as will be discussed elsewhere.

4. Results

Chemical vapor deposition in conjunction with vacuum annealing yields detached crystalline MgO cubes of the size ranging between 3 and 10 nm. These nanocubes exhibit clearly developed edges and have a high concentration of corner sites.[17,30]

The photoluminescence (PL) spectra of MgO nanocubes, before and after hydroxylation, are shown in Figure 2. The broad and asymmetric photoluminescence emission feature has a

(36) Sterrer, M.; Berger, T.; Diwald, O.; Knözinger, E. *J. Am. Chem. Soc*. **2003**, *125*, 195.
(37) Knözinger, E.; Diwald, O.; Sterrer, M. *J. Mol. Catal. A Chem.* **2000**, *162*, 83.
(38) *GRAMS/32 Spectral NotebaseTM*, Version 4.01; Galactic Industries Corporation: Waltham, MA, 1991−1996.
(39) (a) Sushko, P. V.; Shluger, A. L.; Catlow, C. R. A. *Surf. Sci.* **2000**, *450*, 153. (b) Sushko, P. V.; Gavartin, J. L.; Shluger, A. L. *J. Phys. Chem. B* **2002**, *106*, 2269.
(40) Trevisanutto, P. E.; Sushko, P. V.; Shluger, A. L.; Beck, K. M.; Henyk, M.; Joly, A. G.; Hess, W. P. *Surf. Sci.* **2005**, *593*, 210.
(41) Sulimov, V. B.; Sushko, P. V.; Edwards, A. H.; Shluger, A. L.; Stoneham, A. M. *Phys. Rev. B* **2002**, *66*, 024108.
(42) Dick, B. G.; Overhauser, A. W. *Phys. Rev.* **1958**, *112*, 90.
(43) Frisch, M. J.; et al. *Gaussian 98*, revision A.7; Gaussian, Inc.: Pittsburgh, PA, 1998.
(44) Becke, A. D. *J. Chem. Phys.* **1993**, *98*, 5648.
(45) Lee, C.; Yang, W.; Parr, R. G. *Phys. Rev. B* **1988**, *37*, 785.
(46) Wadt, W. R.; Hay, P. J. *J. Chem. Phys.* **1985**, *82*, 284.

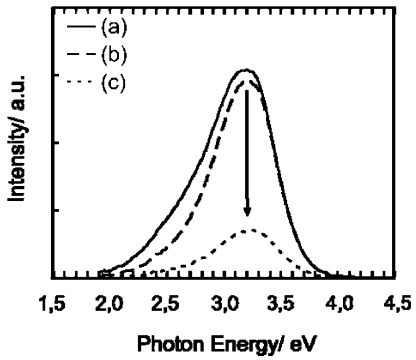

Figure 2. Photoluminescence emission spectra of MgO nanocubes induced by the photoexcitation with 4.6 eV light: (a) dehydroxylated material at $p < 10^{-5}$ mbar (b) after subsequent H_2 addition (10 mbar) and (c) after 20 min of UV exposure to 4.6 eV light in a H_2 atmosphere.

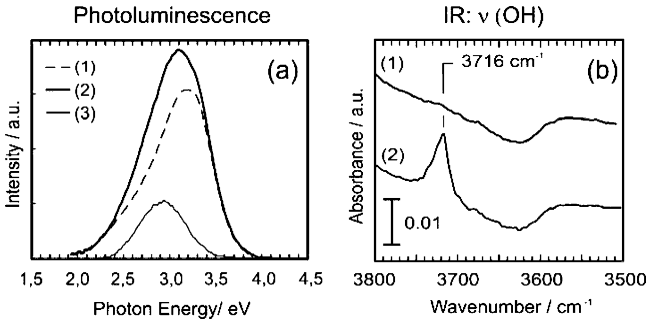

Figure 3. Photoluminescence emission spectra of MgO nanocubes induced by photoexcitation with 4.6 eV light (a) and corresponding IR spectra (b) measured at $p < 10^{-5}$ mbar: (1) dehydroxylated material; (2) after protonation of low-coordinated surface anions via H_2/UV exposure and subsequent vacuum treatment at $T = 870$ K; (3) difference spectrum: (2)−(1).

maximum at 3.2 ± 0.1 eV (Figure 2a) and is specific to dehydroxylated MgO material. This PL band also exhibits a low-energy tail, which extends to 2.0 eV. When dehydroxylated MgO cubes are exposed to H_2 gas (Figure 2b), this tail becomes attenuated, which shifts the maximum of the PL band to slightly higher energies. The present observation is consistent with an earlier photoluminescence study on high surface area MgO,[47] where this low-energy tail has been attributed to specific surface elements, which heterolytically activate H_2.[48] With respect to MgO nanocubes, the maximum surface concentration of such sites was found to be 3% of a nanoparticle monolayer.[49]

During the first few minutes of UV exposure in an H_2 atmosphere the 3.2 eV band maintains its intensity, whereas longer UV exposure times result in a significant depletion of the emission intensity. This is demonstrated by a photoluminescence spectrum, which was acquired after 20 min long UV exposure (Figure 2c). Surface reactions that occur under such experimental conditions are described in detail elsewhere.[34,50] These include homolytic H_2 splitting at oxygen-terminated corner sites[36] as well as formation of surface-trapped electrons, i.e., color centers,[51−53] with distinct optical absorption in the UV−vis region.[50,54] We attribute the PL intensity loss (Figure 2c) to light absorption by such UV−vis active surface products.

Vacuum annealing of the sample at 870 K removes surface color centers, surface hydrides, and most of the hydroxyls. The remaining hydroxyls give rise to an IR band at 3716 cm^{-1} (curve 2 in Figure 3b) and are attributed to oxygen-terminated corners.[55,56] Our theoretical calculations suggest that proton binding to 3C oxygen ions is about 1 eV stronger than that to 4C oxygens and 1.5 eV stronger than that to 5C oxygens. On this basis, we conclude that after the hydroxylation−dehydroxylation procedure protons attached to oxygen-terminated corner sites represent the predominant type of hydrogen defects at the surface of MgO nanocubes.

The photoluminescence emission spectra obtained for dehydroxylated MgO nanocrystals and for those with isolated surface hydroxyls are shown in Figure 3a as curves (1) and (2), respectively, and the corresponding IR spectra are plotted in Figure 3b. The overall photoluminescence emission is clearly enhanced after the partial hydroxylation. In addition, the maximum of the overall emission feature shifts to energies below 3.2 eV. The difference between the emission spectra obtained before and after selective hydroxylation reveals its effect on the surface electronic properties of MgO nanocubes: in addition to the original emission band centered at 3.2 eV, which apparently has not suffered any significant loss of intensity, a new symmetric emission feature at 2.9 eV emerges (curve 3 in Figure 3a). Subsequent sample annealing at 1170 K or higher temperatures leads to a complete dehydroxylation of the entire sample surface, eliminates the contribution at 2.9 eV, and restores the original emission band and the original IR spectrum shown with curves (1) in Figures 3a and 3b, respectively. Such changes of both PL emission and IR absorptions in the OH stretching region are reversible and have been reproduced over many cycles of the partial hydroxylation and thermal annealing. On each cycle the PL and IR spectra fully correlate with each other. We, therefore, assign the 2.9 eV PL band to the most stable surface hydroxyl groups.

For acquisition of the excitation data, we carried out a systematic fitting analysis for both 3.2 ± 0.1 and 2.9 ± 0.1 eV PL bands. Emission was stimulated using monochromatic excitation light in the energy range 4.0−5.2 eV.[57] The resulting spectra were recorded and then submitted to a curve-fitting routine. Essentially, two Gaussian profiles at 3.2 and 2.9 eV with a full-width at half-maximum (fwhm) of 0.7 eV fit the entire set of emission spectra. Intensities for the 3.2 and 2.9 eV bands were determined via band integration analysis and plotted as a function of excitation energy in Figure 4 with open and closed circles, respectively. For comparison a diffuse reflectance

(47) Coluccia, S.; Barton, A.; Tench, A. J. *J. Chem. Soc., Faraday Trans. 1* **1981**, *77*, 2203.
(48) Gribov, E. N.; Bertarione, S.; Scarano, D.; Lamberti, C.; Spoto, G.; Zecchina, A. *J. Phys. Chem. B* **2004**, *108*, 16174.
(49) Berger, T.; Schuh, J.; Sterrer, M.; Diwald, O.; Knözinger, E. *J. Catal.* **2007**, *247*, 61.
(50) Sterrer, M.; Berger, T.; Stankic, S.; Diwald, O.; Knözinger, E. *ChemPhysChem* **2004**, *5*, 1695.
(51) Chiesa, M.; Paganini, M. C.; Giamello, E.; Murphy, D. M.; Di Valentin, C.; Pacchioni, G. *Acc. Chem. Res.* **2006**, *39*, 861.
(52) Chiesa, M.; Paganini, M. C.; Giamello, E.; Murphy, D. M.; Di Valentin, C.; Del Vitto, A.; Pacchioni, G. *J. Phys. Chem. B* **2005**, *109*, 7314.
(53) Sterrer, M.; Fischbach, E.; Risse, T.; Freund, H.-J. *Phys. Rev. Lett.* **2005**, *94*, 186101.
(54) Berger, T.; Sterrer, M.; Diwald, O.; Knözinger, E. *J. Phys. Chem. B* **2004**, *108*, 7280.
(55) Different from previous studies carried out at room temperature,[36] where no annealing procedure has been applied, surface-trapped electrons and surface hydrides, which can influence the position of the OH stretching band, are absent in the present case. This may explain the shift of the band position from[36] 3698 to 3716 cm^{-1} in this work (Figure 3b).
(56) Knözinger, E.; Jacob, K.-H.; Singh, S.; Hofmann, P. *Surf. Sci.* **1993**, *290*, 388.
(57) There is no significant photoluminescence emission when the excitation energies are below 4.0 eV.

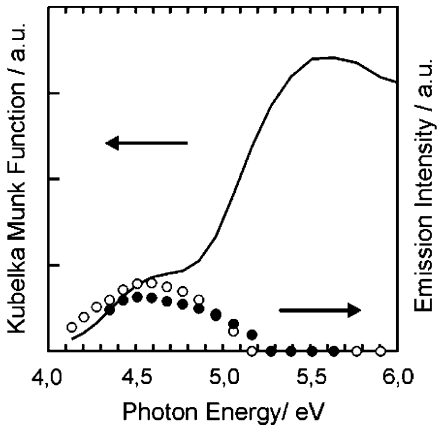

Figure 4. Absorption spectrum of dehydroxylated MgO nanocubes (solid line), the excitation spectrum of the 3.2 ± 0.1 eV emission (open circles) and 2.9 ± 0.1 eV emission (full circles) obtained by band fitting. The lack of data points related to the 2.9 eV emission is due to the overlap between the 2.9 eV emission feature and the unfiltered excitation beam.[62]

spectrum measured for the fully dehydroxylated MgO nanocubes is also shown in Figure 4 (solid line). The excitation spectrum of the 3.2 eV emission band has a maximum at 4.6 eV, which coincides with the low-energy shoulder of the optical absorption of MgO nanocubes that has been attributed to three-coordinated oxygen anions.[17] Interestingly, the excitation spectrum of the 2.9 eV emission band (Figure 4, full circles) closely follows that of the 3.2 eV band and also peaks at 4.6 eV.

5. Discussion

Our results demonstrate that the photoemission at 2.9 ± 0.1 eV is linked to surface defects formed by protonation of oxygen-terminated corner sites and is excited by 4.6 eV light. At the same time, optical absorption at 4.6 eV has been assigned to the electronic excitation of nonprotonated 3C oxygen anions.[15,17,22,30] It, therefore, appears contra-intuitive that both emission bands have nearly identical excitation spectra, even though protonation of 3C anions induces a strong perturbation that significantly modifies their local atomic and electronic structures and should affect the position of the 4.6 eV absorption band. To reveal the proton-induced changes in the optical absorption spectrum of an oxygen-terminated corner, we have calculated the energies and the electronic structures of 15 lowest optical transitions associated with oxygen-terminated corners, both protonated and nonprotonated. Importantly, the QM cluster used in this work includes ions of all coordination numbers; i.e., it represents the corner site as a topological feature rather than a single ion of a specific coordination.

We note that the excitation spectra of the 2.9 and 3.2 eV PL bands are matching the optical absorption band at 4.6 eV in both position of the maximum and the bandwidth.[15,17,18] We, therefore, can discuss the nature of the excitation spectra in terms of optical absorption of the corresponding surface sites. The excitation energies and corresponding relative intensities calculated for the nonprotonated and protonated oxygen corners are shown in Figures 5a and 5b, respectively. In the case of the nonprotonated corner, the lowest energy transitions are dominated by the electron transfer from 2p states of the 3C oxygen (Figure 6a) to the lowest unoccupied molecular orbital (LUMO state) delocalized over three neighboring 4C Mg ions (Figure 6b). The lowest transition at 3.7 eV involves a 2p state associated

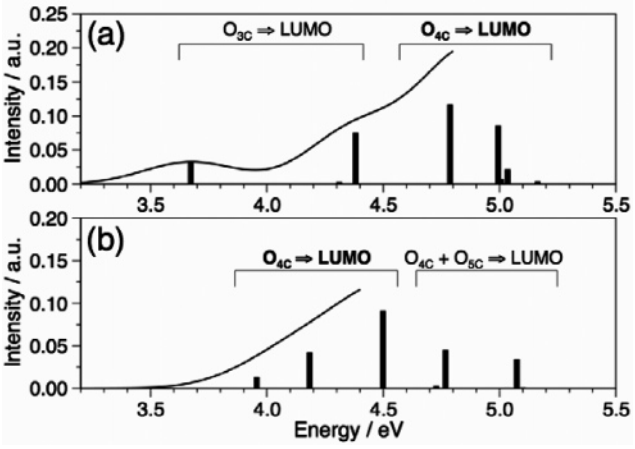

Figure 5. Optical absorption of oxygen-terminated corners: (a) nonprotonated and (b) protonated sites. The position and height of vertical bars indicate calculated excitation energies and relative intensities of the optical transitions, respectively. The thin solid line shows the convolution of Gaussian-type functions (with dispersion of 0.2 eV) representing transitions in the low-energy part of each spectrum, which corresponds to the 4−4.5 eV range in Figure 4. The qualitative nature of the transitions is also indicated to illustrate the magnitude of the red shift.

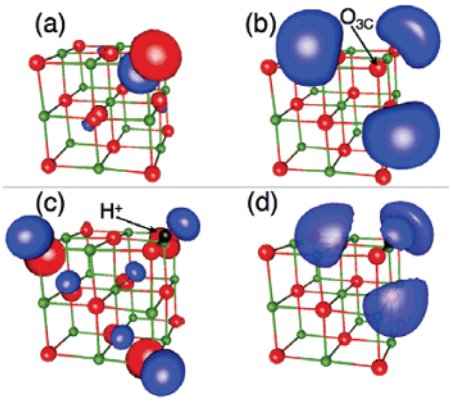

Figure 6. Molecular orbitals involved in characteristic optical transitions: (a) and (b) are the HOMO and LUMO states at a nonprotonated oxygen-terminated site, respectively; (c) a linear combination of 2p states associated with 4C oxygen ions (applies to both protonated and nonprotonated systems); (d) the LUMO state at a protonated corner site.

with 3C oxygen and oriented along ⟨111⟩ shown in Figure 6a, while two other transitions, which involve 2p states oriented perpendicular to ⟨111⟩ (not shown), are found at 4.4 eV. Prominent 4C→LUMO transitions, found at 4.8 eV and around 5.0 eV, correspond to the charge transfer from differently oriented 2p states of edge O ions in the vicinity of the oxygen corner site (Figure 6c). The 5C→LUMO transitions were outside of the calculated range of excitation energies considered here.

The protonation of a 3C oxygen site modifies the nature of the absorption spectrum (see Figure 5b): the corner O ion becomes effectively four-coordinated (4C) and the H^+ ion provides a strong positive electrostatic potential, which stabilizes the 2p states of the corner oxygen. Consequently, all transitions associated with the states of the corner O, e.g., that shown in Figure 6a, disappear from the low-energy part of the absorption spectrum and the transitions associated with the states of the 4C edge O ions (Figure 6c) become dominant. At the same time, the electrostatic potential produced by H^+ ion polarizes the LUMO state (Figure 6d) and shifts the 4C→LUMO transitions to lower energies. In particular, the excitation energies of these transitions shift from 4.8 to 4.2 eV and from 5.0 to 4.5 eV. In

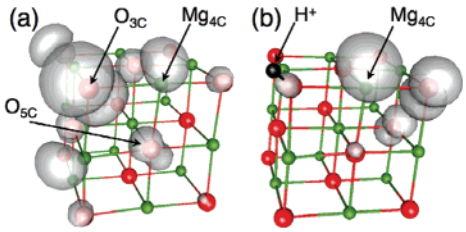

Figure 7. Spin densities calculated for the relaxed triplet states: (a) nonprotonated and (b) protonated oxygen-terminated corners shown in the same perspective. The spin-density distribution in (a) follows the C_3 symmetry of the corner site, while the spin-density distribution in (b) is of lower symmetry due to an asymmetric relaxation of the corner OH^- group (the relaxation is not shown).

addition, higher energy 4C→LUMO transitions with a small contribution from 5C oxygen states appear at 4.8 and 5.1 eV.

Therefore, the protonation of 3C oxygen sites not only removes the absorption due to 3C site per se but also shifts the absorption bands associated with the nearby 4C oxygen sites to lower energies. As a result, a strong absorption intensity remains in the region of 4.0−4.8 eV even after the protonation.

Accurate calculations of the photoluminescence spectra require detailed knowledge of the potential energy surfaces of the excited states and relevant relaxation rates. In its entirety this problem is extremely demanding. However, one can obtain additional insight into the electronic structure of the excited states and the shift of the photoluminescence energies by calculating the potential energy minimum of the lowest triplet state. Then the luminescence energy can be calculated as the energy of the triplet → singlet transition. The spin densities calculated for the triplet states are shown in Figure 7. The lowest triplet state in the case of the nonprotonated corner relaxes into a symmetrical configuration (Figure 7a), while in the case of the protonated corner such relaxation is asymmetric and, therefore, the distribution of the spin density is qualitatively different (Figure 7b). In each case the photoluminescence energy (E_{PL}) has been calculated as the difference in the total energies obtained for the corresponding triplet and singlet electronic states and the atomic configuration of the triplet state. The calculated values of E_{PL} are 2.6 eV for nonprotonated and 2.3 eV for protonated corners. The difference between these values matches the energy difference between the measured positions of the PL maxima at 3.2 and 2.9 eV, respectively. We note, however, that these luminescence energies correspond to the lowest but not to the most intense transitions excited at ∼4.6 eV.

6. Summary and Conclusions

We present a combined experimental and theoretical study of optical properties of clean and partially hydroxylated MgO nanocubes. The site-selective hydroxylation procedure was designed so as to induce a specific chemical modification: attachment of a proton to three-coordinated oxygen sites. The 2.9 eV photoluminescence band observed on hydroxylated samples was associated with such modified sites. The excitation spectrum of the 2.9 eV PL band peaks at the same energy (4.6 eV) as the optical absorption band previously assigned to nonprotonated three-coordinated oxygen sites. Our results suggest that this is a coincidence, which is determined primarily by two factors. First, the optical absorption band with the maximum at 4.6 eV, attributed to the three-coordinated oxygens, contains a significant contribution of the $O_{4C} \Rightarrow Mg_{4C}$ charge transfer due to the 4C ions in the immediate vicinity of the corner sites. According to the theoretical calculations, these ions absorb photons of energies as low as 4.8 eV, which is much lower than 5.7 eV usually associated with the optical absorption of 4C ions. We therefore suggest that the 4.6 eV absorption band should be assigned not to three-coordinated ions alone but to the corner topological feature as a whole. Second, the protonation of a 3C oxygen site induces a strong red shift of the excitation energies attributed to $O_{4C} \Rightarrow Mg_{4C}$ transitions. As a result, the intensity of the optical absorption in the region of 4−5 eV remains strong and gives rise to the new photoluminescence feature. Although the experimental techniques used in this work do not allow us to clearly distinguish between simple corners and other more complex types of sites terminated with 3C oxide ions, we suggest that these effects apply to the whole family of various 3C sites.

Both of these results are generic and apply equally to rough insulating surfaces and nanostructures and shed new light on the photochemical processes in these systems.[58−61] In particular, associating the optical absorption bands with individual ions or ions of specific coordination may lead to erroneous conclusions. Instead, surface topological features should be understood as materials building blocks. Finally, we find that in spite of a significant effect on the nature of optical transitions, the protonation may only slightly affect the measured absorption spectrum. This effect should be especially taken into account in cases where hydroxylation of the samples takes place in the course of an experiment.

Acknowledgment. We would like to thank G. Pacchioni, M. Chiesa, E. Giamello, and K. McKenna for their comments on the manuscript. The experimental work carried out by the Vienna group was financially supported by Fonds zur Förderung der Wissenschaftlichen Forschung (FWF) P 17770-N11, which is gratefully acknowledged. P.V.S. is supported by the Grant-in-Aid for Creative Scientific Research (Grant No. 16GS0205) from the Japanese Ministry of Education, Culture, Sports, Science and Technology. P.E.T. was supported by the Department of Energy, Divisions of Chemical Sciences of the Office of Basic Energy Sciences. Pacific Northwest National Laboratory is operated for the U.S. Department of Energy by Battelle. Travel support for the Vienna-London cooperation stems from the ESF (COST action D41 "Inorganic oxide surfaces and interfaces"). The calculations were carried out by the London group on the UCL Central Computing Cluster and HPCx facility through Materials Chemistry consortium.

Supporting Information Available: Complete ref 34 and figures illustrating the model setup used in theoretical calculations. This material is available free of charge via the Internet at http://pubs.acs.org.

JA0736055

(58) Thompson, T. L.; Yates, J. T. *Chem. Rev.* **2006**, *106*, 4428.
(59) Osgood, R. *Chem. Rev.* **2006**, *106*, 4379.
(60) Hess, W. P.; Joly, A. G.; Beck, K. M.; Henyk, M.; Sushko, P. V.; Trevisanutto, P. E.; Shluger, A. L. *J. Phys. Chem. B* **2005**, *109*, 19563.
(61) Grätzel, M. *Inorg. Chem.* **2005**, *44*, 6841.
(62) This problem does not apply for the 3.2 eV emission where a cut-off filter, which eliminates stray light with $h\nu > 3$ eV, can be used.